CHARGED-CURRENT ELECTRON NEUTRINOS IN MICROBOONE

ICHEP, Neutrino Physics

Wouter Van De Pontseele – On behalf of the MicroBooNE collaboration
woutervdp@g.harvard.edu

July 28, 2020

The measurement of the ν_e electron kinematics is crucial towards understanding the nature of the observed excess of low-energy electromagnetic-like events at MiniBooNE.

1. Cosmic rejection.
2. ν_e's in MicroBooNE.
3. Electron identification.
4. ν_e CC Event selection.
5. Sideband results & near-future.

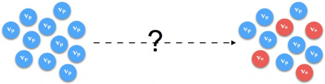

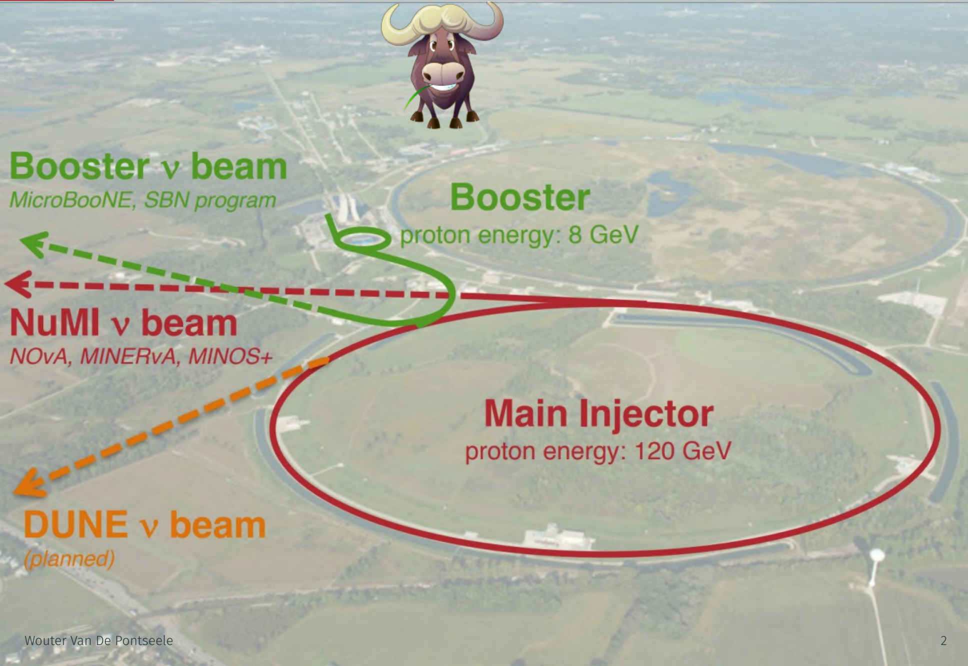
Booster ν beam
MicroBooNE, SBN program
Booster
proton energy: 8 GeV
NuMI ν beam
NOvA, MINERvA, MINOS+
Main Injector
proton energy: 120 GeV
DUNE ν beam
(planned)

The MicroBooNE experiment

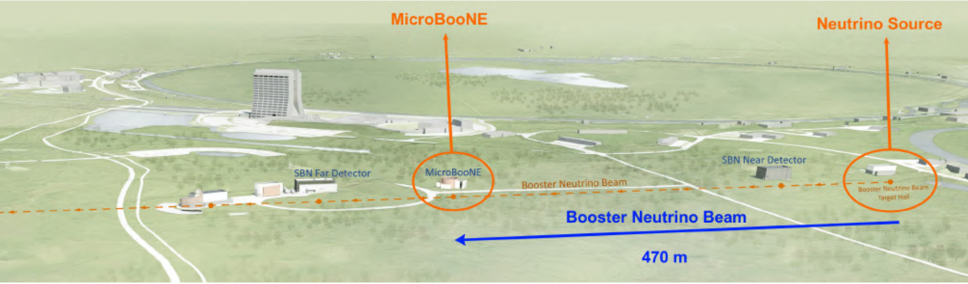

Electron Neutrino Physics

- Electron identification in Liquid Argon Time Projection Chambers.
- Further investigate the **low-energy excess** observed by MiniBooNE [1].
- Measuring the $\approx 0.5\,\%$ ν_e component in a muon neutrino beam.
- **Cross-section** measurements on argon [2, 3].

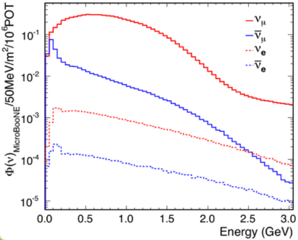

Detector Understanding

- Signal processing [5, 6].
- Detector calibration [7].
- Pandora event reconstruction [8].

Background rejection

- Cosmic activity [11].
- Muon neutrino backgrounds.

Search for Electron neutrinos

- Particle identification:
  - Showers: e/γ
  - Tracks: p/μ
- Event topologies.
- Kinematics of the electron.

Systematic Uncertainties

- Neutrino flux from beam.
- Cross-section modelling (Genie) [9].
- Secondary Interactions (GEANT).
- Detector effects [10].

Detector Understanding

- Signal processing [5, 6].
- Detector calibration [7].
- Pandora event reconstruction [8].

Background rejection

- Cosmic activity [11].
- Muon neutrino backgrounds.

Systematic Uncertainties

- Neutrino flux from beam.
- Cross-section modelling (Genie) [9].
- Secondary Interactions (GEANT).
- Detector effects [10].

Search for Electron neutrinos

- Particle identification:
  - Showers: e/γ
  - Tracks: p/μ
- Event topologies.
- Kinematics of the electron.

Talk by Ralitsa Sharankova: The MicroBooNE Experiment, Operation, Performance and Upgrade of Present Detectors

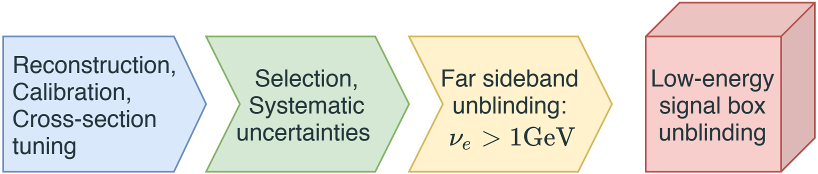

- MicroBooNE follows a **blind analysis** strategy to investigate the MiniBooNE result.
- Reconstruction and selection being developed on an unbiased sub-set corresponding to 5×10^{19} protons-on-target.
- **On the cusp of unblinding** a 3-year data-set, containing 7×10^{20} protons-on-target.

ν_e's in MicroBooNE: Steps towards unblinding

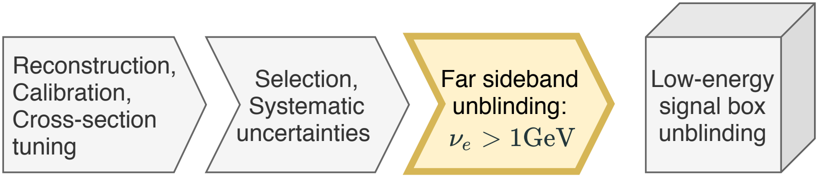

- MicroBooNE follows a **blind analysis** strategy to investigate the MiniBooNE result.
- Reconstruction and selection being developed on an unbiased sub-set corresponding to 5×10^{19} protons-on-target.
- **On the cusp of unblinding** a 3-year data-set, containing 7×10^{20} protons-on-target.

Brand new results shown on sideband containing electron neutrinos with a reconstructed energy above 1 GeV!

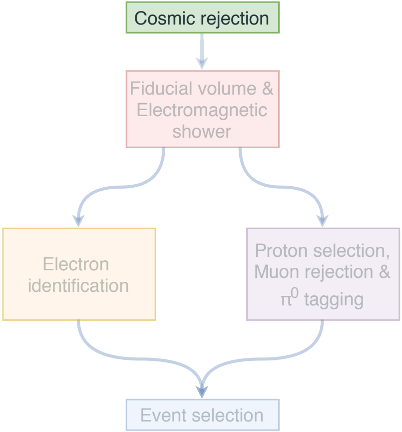
Cosmic rejection
Fiducial volume & Electromagnetic shower
Electron identification
Proton selection, Muon rejection & π^0 tagging
Event selection

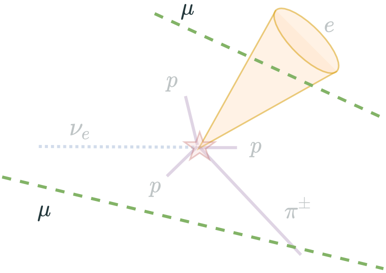
μ
e
p
ν_e
p
p
μ
$\pi^\pm$

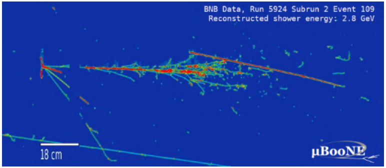
BNB Data, Run 5924 Subrun 2 Event 109
Reconstructed shower energy: 2.8 GeV
18 cm
µBooNE

- MicroBooNE is a surface detector.
- 5 kHz cosmic muon rate.
- Approximately 24 muons per triggered event.
- Modelled using Off Beam data.

→ Cosmic rejection tools as
first selection steps in all analyses!

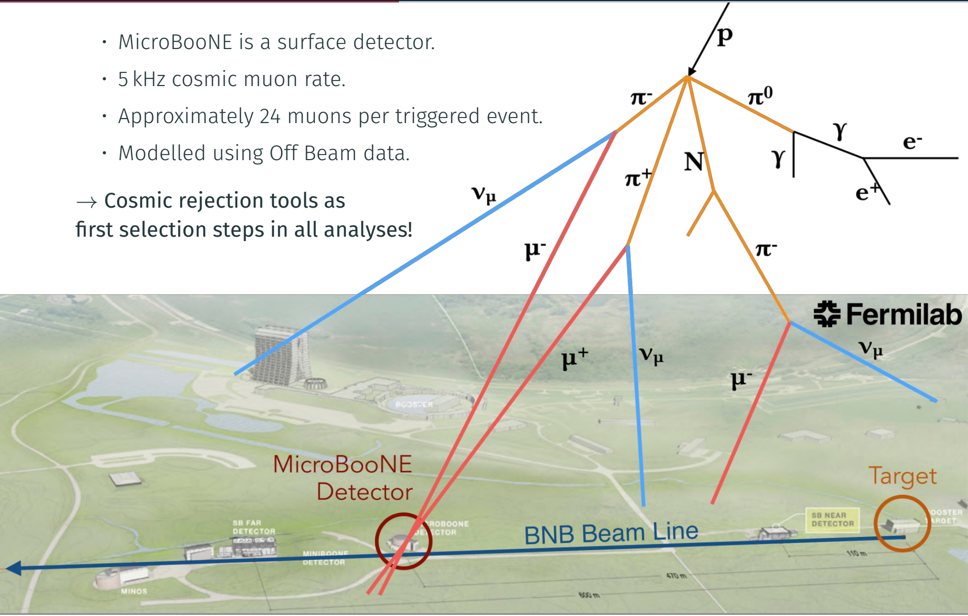

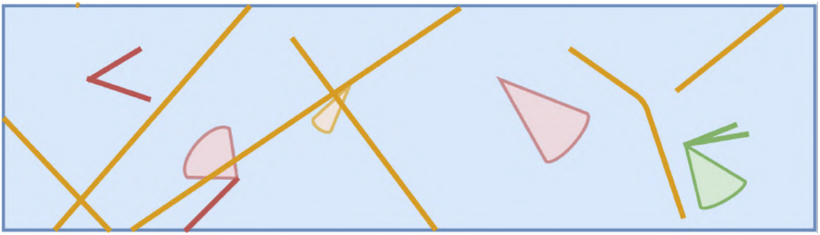

1. Require **light in-time** with the accelerator trigger.
2. Remove tracks geometrically crossing the detector.
3. Identify muons stopping in the TPC using calorimetry.

Cosmic rejection tools

1. Require **light in-time** with the accelerator trigger.
2. Remove tracks geometrically crossing the detector.
3. Identify muons stopping in the TPC using calorimetry.
4. **Match the** light signal **to** TPC activity in charge and position.

Cosmic rejection efficiency for charged-current interactions

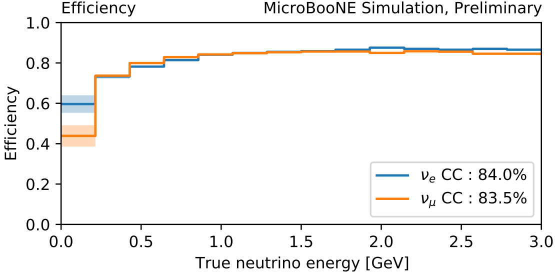

1. Require **light in-time** with the accelerator trigger.
2. Remove tracks **geometrically crossing** the detector.
3. Identify **muons stopping in the TPC** using calorimetry.
4. **Match the light signal to TPC activity** in charge and position.

Neutrino efficiency of ≈84 % and cosmic rejection of 99.8 %.

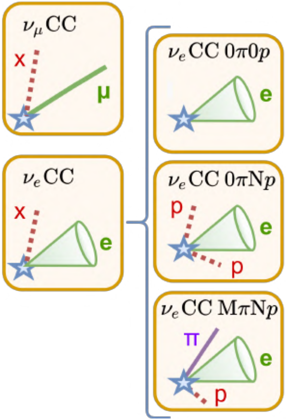

Talk by Raquel Castillo Fernandez:
Recent Cross-section Measurements from MicroBooNE.

⇒ **Argon is complicated and cross-section modelling carries large uncertainties.**

At the Booster Neutrino Beam, $< E(\nu_e) > \approx 1\,\text{GeV}$**,**
A variety of final states are expected:

- **1**e**0**p**0**π: dominant below ≈0.3 GeV.
- **1**eNp**0**π
- **1**eNpMπ: dominant above ≈2 GeV.

⇒ **Important to perform an inclusive measurement to support observations in low-energy or exclusive channels.**

⇒ Talk by David Caratelli
The status of the low-energy excess.

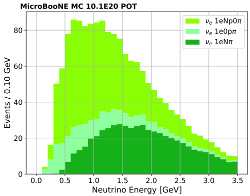

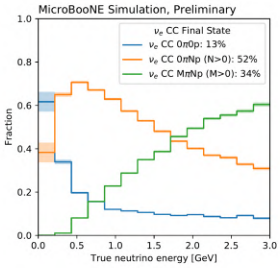

Talk by Raquel Castillo Fernandez:
Recent Cross-section Measurements from MicroBooNE.

$\Rightarrow$ **Argon is complicated and cross-section modelling carries large uncertainties.**

At the Booster Neutrino Beam, $< E(\nu_e) > \approx 1\,\text{GeV}$**,**
A variety of final states are expected:

- **1e0p0π**: dominant below ≈0.3 GeV.
- **1eNp0π**
- **1eNpMπ**: dominant above ≈2 GeV.

$\Rightarrow$ **Important to perform an inclusive measurement to support observations in low-energy or exclusive channels.**

$\Rightarrow$ Talk by David Caratelli
The status of the low-energy excess.

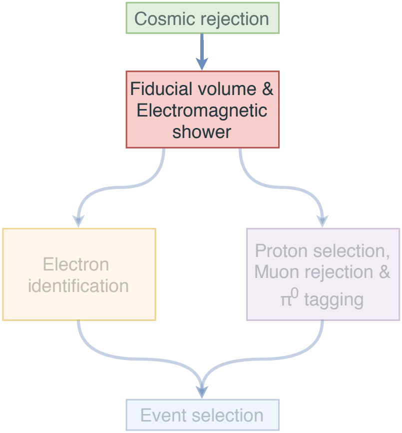
Cosmic rejection
Fiducial volume & Electromagnetic shower
Electron identification
Proton selection, Muon rejection & π^0 tagging
Event selection

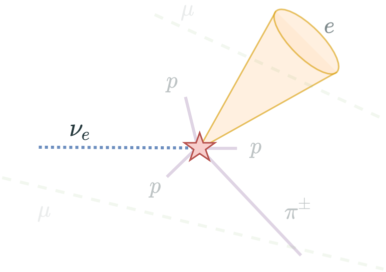
μ
e
p
ν_e
p
p
μ
$\pi^{\pm}$

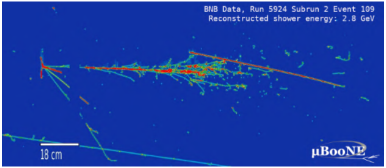
BNB Data, Run 5924 Subrun 2 Event 109
Reconstructed shower energy: 2.8 GeV
18 cm
µBooNE

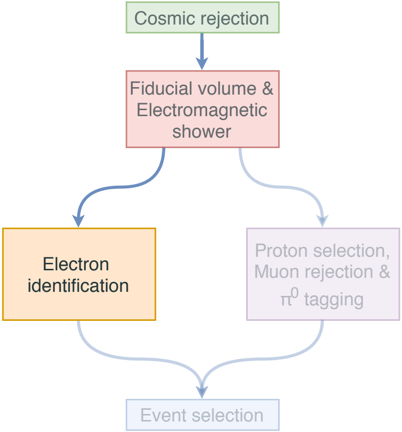
Cosmic rejection
Fiducial volume & Electromagnetic shower
Electron identification
Proton selection, Muon rejection & π^0 tagging
Event selection

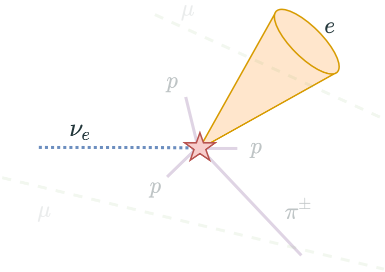
μ
e
p
ν_e
p
p
μ
$\pi^{\pm}$

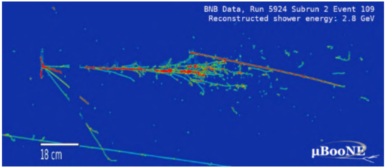
BNB Data, Run 5924 Subrun 2 Event 109
Reconstructed shower energy: 2.8 GeV
18 cm
µBooNE

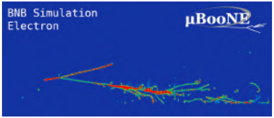

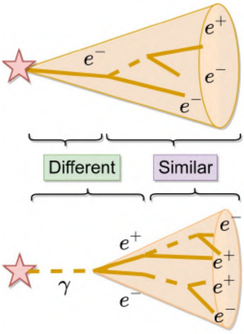

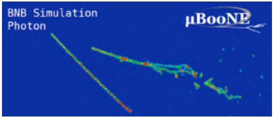

- e/γ separation enabled by **differences** in the **start** of the electromagnetic **shower**.
- **Demonstrated using photons** from π^0 decay [12].

1. dE/dx
2. Detached shower start point

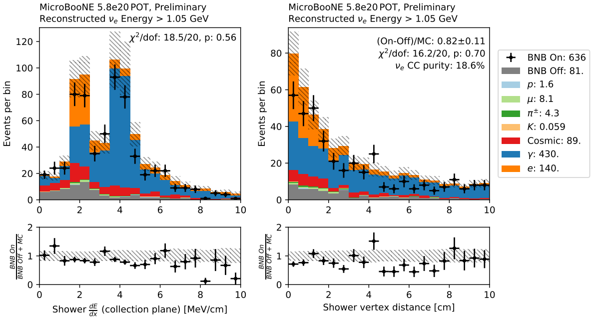

Particle Identification: Photons vs Electrons

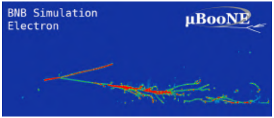

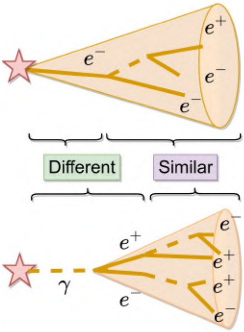

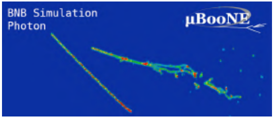

- e/γ separation enabled by **differences** in the **start** of the electromagnetic **shower**.
- **Demonstrated using photons** from π^0 decay [12].

Boosted decision tree used for shower classification:

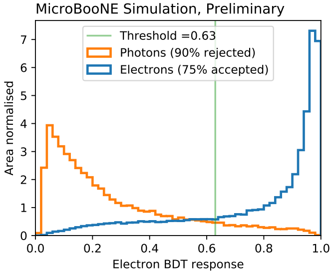

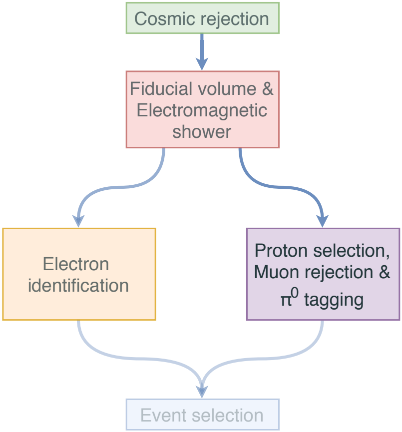

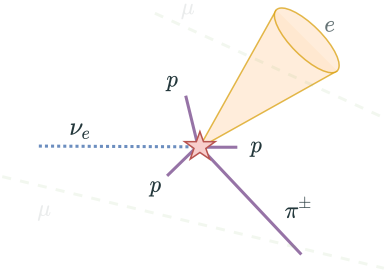

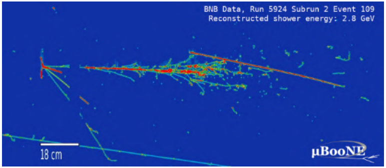

Identification the other objects in the event.
Are these tracks protons or muon?

Particle Identification: Protons vs Muons

Difference in energy losses due to particle mass (**Bethe-Bloch**)

- **Muons**: Minimum ionising + short Bragg peak.
- **Protons**: Heavier and slower → higher energy losses.
- **Detector anisotropies** complicate the picture.

Likelihood ratio as test-statistic:

$$\mathcal{T}(dE/dx, segment, \theta) = \frac{\mathcal{L}(muon \mid dE/dx, segment, \theta)}{\mathcal{L}(proton \mid dE/dx, segment, \theta)}$$

Combines all **three wire planes**:

$$\mathcal{L}(U, V, Y) = \mathcal{L}(U) \times \mathcal{L}(V) \times \mathcal{L}(Y)$$

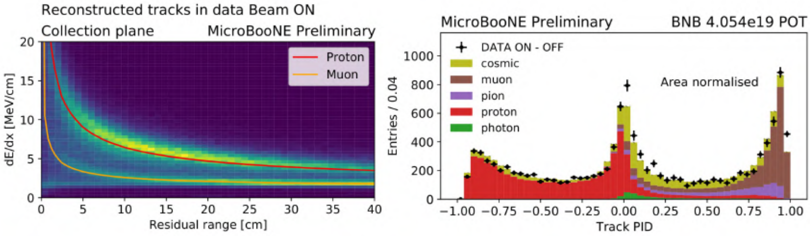

ν_e CC Inclusive event selection

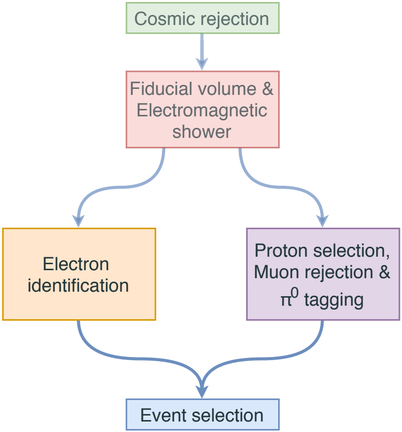

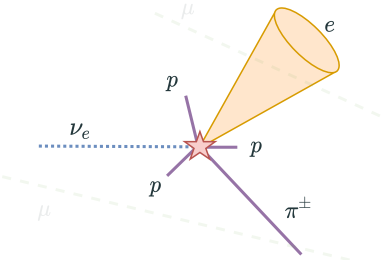

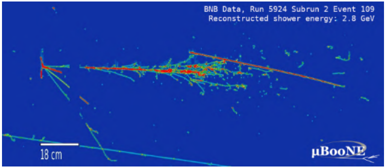

The final event selection builds on top of
the identification of the different particles in the interactions.

- Low electron neutrino purity after pre-selection: $\mathcal{O}(5\%)$.
- Main backgrounds after pre-selection are muon neutrinos.
- Use **gradient boosted decision trees** (XGBoost).
- Toughest background to reduce are **muon neutrinos with** π^0.

Final selection with a ν_e CC purity of 50 %+
and a wide variety of shower energies and vertex multiplicities.

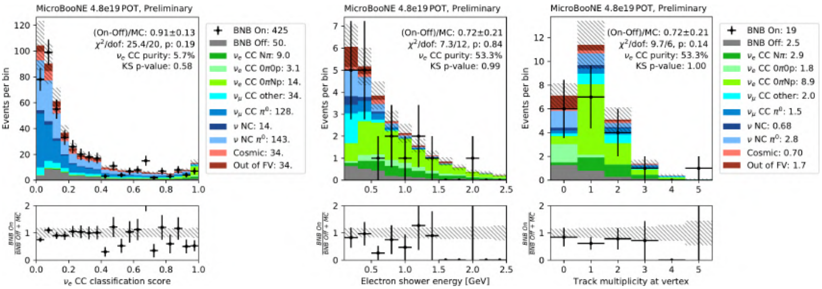

- **ν_e CC efficiency of** 18 %.
  We select events in all three categories, but not tailored for low-energy search.

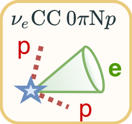

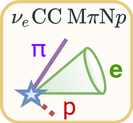

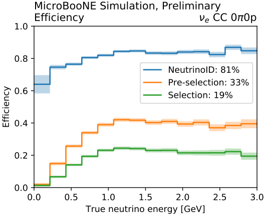

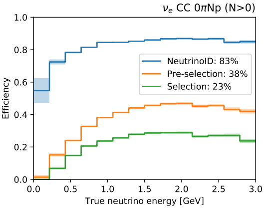

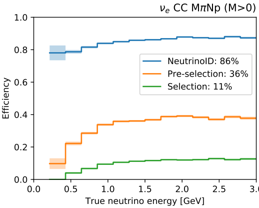

- ν_e CC efficiency of 18 %.
  We select events in all three categories, but not tailored for low-energy search.
- Resolution of electrons kinematics.

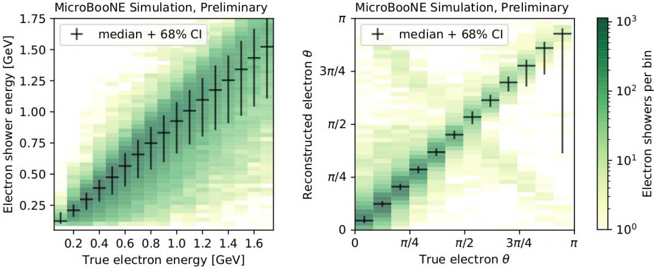

Electron energy reconstructed within ≈20 %

≈ 3° degree resolution on the angle with respect to the beam direction.

- ν_e CC efficiency of 18 %.
  We select events in all three categories, but not tailored for low-energy search.
- Resolution of electrons kinematics.
- Sideband results. ν_e-pure high-energy sample demonstrates good agreement with high statistics. The energy threshold is lowered gradually towards full unblinding.

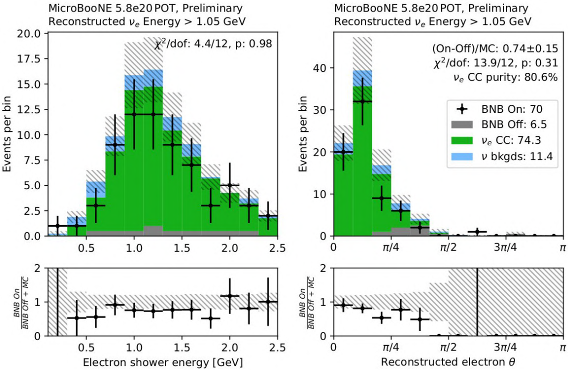

Conclusion & Near-future

Electron neutrinos in MicroBooNE

- Fully automatic ν_e reconstruction and selection in a LArTPC.
- Shower (e/γ) and track (p/μ) identification.
- Efficiency of 18 % with purity of 50 %+ for ν_e CC interactions.
- Wide variety of final states and electron kinematics.

More results soon!

- Concurrent effort ongoing with the NuMI beam [13].
- Progress towards **measurements** of the $\boldsymbol{\nu_e}$ **content in the BNB beam** and the $\boldsymbol{\nu_e}$ **cross-section** on Argon.

MICROBOONE-NOTE-1085-PUB

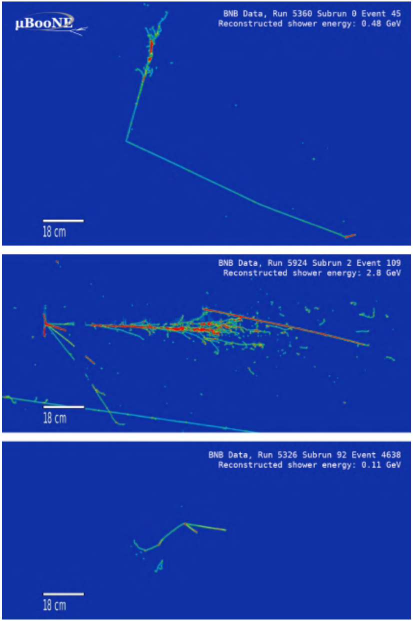

Thank you!
& Questions

References

- MiniBooNE Collaboration. “Significant Excess of Electronlike Events in the MiniBooNE Short-Baseline Neutrino Experiment”. In: *Phys. Rev. Lett.* 121 (2018), p. 221801. DOI: 10.1103/PhysRevLett.121.221801. arXiv: 1805.12028.
- MicroBooNE Collaboration. “First Measurement of Inclusive Muon Neutrino Charged Current Differential Cross Sections on Argon at $E_\nu \sim 0.8\ \mathrm{GeV}$ with the MicroBooNE Detector”. In: *Phys. Rev. Lett.* 123 (2019), p. 131801. DOI: 10.1103/PhysRevLett.123.131801. arXiv: 1905.09694.
- MicroBooNE Collaboration. “First measurement of ν_μ charged-current π^0 production on argon with the MicroBooNE detector”. In: *Phys. Rev. D* 99 (2019), p. 091102. DOI: 10.1103/PhysRevD.99.091102. arXiv: 1811.02700.
- Pedro A.N. Machado, Ornella Palamara, and David W. Schmitz. “The Short-Baseline Neutrino Program at Fermilab”. In: *Annual Review of Nuclear and Particle Science* 69.1 (2019), pp. 363–387. DOI: 10.1146/annurev-nucl-101917-020949.

MicroBooNE Collaboration. "Ionization electron signal processing in single phase LArTPCs. Part I. Algorithm Description and quantitative evaluation with MicroBooNE simulation". In: *JINST* 13.07 (2018), P07006–P07006. ISSN: 1748-0221. DOI: `10.1088/1748-0221/13/07/p07006`. arXiv: `1802.08709`.

"Ionization electron signal processing in single phase LArTPCs. Part II. Data/simulation comparison and performance in MicroBooNE". In: *JINST* 13.07 (2018), P07007. DOI: `10.1088/1748-0221/13/07/P07007`. arXiv: `1804.02583`.

MicroBooNE Collaboration. "Calibration of the charge and energy loss per unit length of the MicroBooNE liquid argon time projection chamber using muons and protons". In: *JINST* 15.03 (2020), P03022–P03022. DOI: `10.1088/1748-0221/15/03/p03022`. arXiv: `1910.02166`.

MicroBooNE Collaboration. "The Pandora multi-algorithm approach to automated pattern recognition of cosmic-ray muon and neutrino events in the MicroBooNE detector". In: *Eur. Phys. J.* C.78 (2018), p. 1. arXiv: `1708.03135`.

MicroBooNE Collaboration. "Neutrino Interaction Model and Uncertainties for MicroBooNE Analyses". In: *MICROBOONE-NOTE-1074-PUB* (2020).

- MicroBooNE Collaboration. “Novel Approach for Evaluating Detector Systematics in the MicroBooNE LArTPC”. In: *MICROBOONE-NOTE-1075-PUB* (2020).
- MicroBooNE Collaboration. “Cosmic Ray Background Rejection with Wire-Cell LArTPC Event Reconstruction in MicroBooNE”. In: *MICROBOONE-NOTE-1084-PUB* (2020).
- “Reconstruction and Measurement of $\mathcal{O}(100)$ MeV Energy Electromagnetic Activity from $\pi^0 \to \gamma\gamma$ Decays in the MicroBooNE LArTPC”. In: *JINST* 15.02 (2020), P02007. DOI: 10.1088/1748-0221/15/02/P02007. arXiv: 1910.02166.
- MicroBooNE Collaboration. “Automated Selection of Electron Neutrinos from the NuMI beam in the MicroBooNE Detector and Prospects for a Measurement of the Charged-Current Inclusive Cross Section”. In: *MICROBOONE-NOTE-1054-PUB* (2018).
- James E. Hill. “An Alternative Analysis of the LSND Neutrino Oscillation Search Data on $\overline{\nu}_\mu \to \overline{\nu}_e$”. In: *Phys. Rev. Lett.* 75 (1995), pp. 2654–2657. DOI: 10.1103/PhysRevLett.75.2654.

MicroBooNE Collaboration. “Deep neural network for pixel-level electromagnetic particle identification in the MicroBooNE liquid argon time projection chamber”. In: *Phys. Rev. D* 99 (2019), p. 092001. DOI: 10.1103/PhysRevD.99.092001. arXiv: 1808.07269.

- Mixing between neutrino flavour and mass eigenstates: PMNS matrix

$$\begin{pmatrix} \nu_e \\ \nu_\mu \\ \nu_\tau \end{pmatrix} = U(\theta_{12}, \theta_{23}, \theta_{13}, \delta_{CP}) = \begin{pmatrix} U_{e1} & U_{e2} & U_{e3} \\ U_{\mu 1} & U_{\mu 2} & U_{\mu 3} \\ U_{\tau 1} & U_{\tau 2} & U_{\tau 3} \end{pmatrix} \begin{pmatrix} \nu_1 \\ \nu_2 \\ \nu_3 \end{pmatrix}$$

- Mixing between neutrino flavour and mass eigenstates: PMNS matrix

$$\begin{pmatrix} \nu_e \\ \nu_\mu \\ \nu_\tau \end{pmatrix} = U(\theta_{12}, \theta_{23}, \theta_{13}, \delta_{CP}) = \begin{pmatrix} U_{e1} & U_{e2} & U_{e3} \\ U_{\mu 1} & U_{\mu 2} & U_{\mu 3} \\ U_{\tau 1} & U_{\tau 2} & U_{\tau 3} \end{pmatrix} \begin{pmatrix} \nu_1 \\ \nu_2 \\ \nu_3 \end{pmatrix}$$

- Propagation through vacuum over a length L for mass eigenstate ν_i:

$$|\nu_i(L)\rangle \approx e^{-i\frac{m_i^2 L}{2E}} |\nu_i(0)\rangle \,.$$

- Mixing between neutrino flavour and mass eigenstates: PMNS matrix

$$\begin{pmatrix} \nu_e \\ \nu_\mu \\ \nu_\tau \end{pmatrix} = U(\theta_{12}, \theta_{23}, \theta_{13}, \delta_{CP}) \approx \begin{pmatrix} 0.8 & 0.5 & 0.1 \\ 0.3 & 0.7 & 0.6 \\ 0.4 & 0.5 & 0.8 \end{pmatrix} \begin{pmatrix} \nu_1 \\ \nu_2 \\ \nu_3 \end{pmatrix}$$

- Propagation through vacuum over a length L for mass eigenstate ν_i:

$$|\nu_i(L)\rangle \approx e^{-i\frac{m_i^2 L}{2E}} |\nu_i(0)\rangle \, .$$

The combination leads to neutrino flavour oscillations!

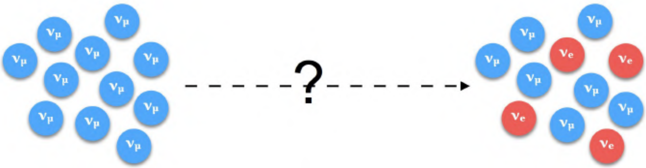

- Let's add a sterile fourth neutrino to the game!

$$\begin{pmatrix} \nu_e \\ \nu_\mu \\ \nu_\tau \\ \boldsymbol{\nu}_S \end{pmatrix} = \begin{pmatrix} U_{e1} & U_{e2} & U_{e3} & U_{\boldsymbol{e4}} \\ U_{\mu 1} & U_{\mu 2} & U_{\mu 3} & U_{\boldsymbol{\mu 4}} \\ U_{\tau 1} & U_{\tau 2} & U_{\tau 3} & U_{\boldsymbol{\tau 4}} \\ U_{\boldsymbol{S1}} & U_{\boldsymbol{S2}} & U_{\boldsymbol{S3}} & U_{\boldsymbol{S4}} \end{pmatrix} \begin{pmatrix} \nu_1 \\ \nu_2 \\ \nu_3 \\ \boldsymbol{\nu_4} \end{pmatrix}$$

- Let's add a sterile fourth neutrino to the game!

$$\begin{pmatrix} \nu_e \\ \nu_\mu \\ \nu_\tau \\ \boldsymbol{\nu}_S \end{pmatrix} = \begin{pmatrix} U_{e1} & U_{e2} & U_{e3} & U_{\boldsymbol{e4}} \\ U_{\mu 1} & U_{\mu 2} & U_{\mu 3} & U_{\boldsymbol{\mu 4}} \\ U_{\tau 1} & U_{\tau 2} & U_{\tau 3} & U_{\boldsymbol{\tau 4}} \\ U_{\boldsymbol{S1}} & U_{\boldsymbol{S2}} & U_{\boldsymbol{S3}} & U_{\boldsymbol{S4}} \end{pmatrix} \begin{pmatrix} \nu_1 \\ \nu_2 \\ \nu_3 \\ \boldsymbol{\nu_4} \end{pmatrix}$$

- Consider experiments where $\frac{E}{L} \approx \Delta m^2_{41}$ and $\Delta m^2_{41} >> \Delta m^2_{21}, \Delta m^2_{32}$.
- If we are only sensitive to electron and muon flavours in the detector:

U_{e4}, $U_{\mu 4}$ and Δm^2_{41}

- Let's add a sterile fourth neutrino to the game!

$$\begin{pmatrix} \nu_e \\ \nu_\mu \\ \nu_\tau \\ \boldsymbol{\nu}_S \end{pmatrix} = \begin{pmatrix} U_{e1} & U_{e2} & U_{e3} & \mathrm{U}_{\boldsymbol{e4}} \\ U_{\mu 1} & U_{\mu 2} & U_{\mu 3} & \mathrm{U}_{\boldsymbol{\mu 4}} \\ U_{\tau 1} & U_{\tau 2} & U_{\tau 3} & \mathrm{U}_{\boldsymbol{\tau 4}} \\ \mathrm{U}_{\mathbf{S1}} & \mathrm{U}_{\mathbf{S2}} & \mathrm{U}_{\mathbf{S3}} & \mathrm{U}_{\mathbf{S4}} \end{pmatrix} \begin{pmatrix} \nu_1 \\ \nu_2 \\ \nu_3 \\ \boldsymbol{\nu}_4 \end{pmatrix}$$

- Consider experiments where $\frac{E}{L} \approx \Delta m^2_{41}$ and $\Delta m^2_{41} >> \Delta m^2_{21}, \Delta m^2_{32}$.
- If we are only sensitive to electron and muon flavours in the detector:

$$\mathrm{U}_{\boldsymbol{e4}}, \mathrm{U}_{\boldsymbol{\mu 4}} \text{ and } \boldsymbol{\Delta}\mathrm{m}^2_{\mathbf{41}}$$

$$P(\nu_e \to \nu_e) = 1 - 4(1 - |\mathrm{U}_{\boldsymbol{e4}}|^2)|\mathrm{U}_{\boldsymbol{e4}}|^2 \sin^2(1.27\boldsymbol{\Delta}\mathrm{m}^2_{\mathbf{41}}\frac{L}{E}) \qquad (\nu_e \text{ disappearance})$$

$$P(\nu_\mu \to \nu_\mu) = 1 - 4(1 - |\mathrm{U}_{\boldsymbol{\mu 4}}|^2)|\mathrm{U}_{\boldsymbol{\mu 4}}|^2 \sin^2(1.27\boldsymbol{\Delta}\mathrm{m}^2_{\mathbf{41}}\frac{L}{E}) \qquad (\nu_\mu \text{ disappearance})$$

$$P(\nu_\mu \to \nu_e) = 4|\mathrm{U}_{\boldsymbol{e4}}|^2|\mathrm{U}_{\boldsymbol{\mu 4}}|^2 \sin^2(1.27\boldsymbol{\Delta}\mathrm{m}^2_{\mathbf{41}}\frac{L}{E}) \qquad (\nu_e \text{ appearance})$$

- Let's add a sterile fourth neutrino to the game!

$$\begin{pmatrix} \nu_e \\ \nu_\mu \\ \nu_\tau \\ \boldsymbol{\nu}_S \end{pmatrix} = \begin{pmatrix} U_{e1} & U_{e2} & U_{e3} & \mathrm{U}_{\boldsymbol{e4}} \\ U_{\mu 1} & U_{\mu 2} & U_{\mu 3} & \mathrm{U}_{\boldsymbol{\mu 4}} \\ U_{\tau 1} & U_{\tau 2} & U_{\tau 3} & \mathrm{U}_{\boldsymbol{\tau 4}} \\ \mathrm{U}_{\mathbf{S1}} & \mathrm{U}_{\mathbf{S2}} & \mathrm{U}_{\mathbf{S3}} & \mathrm{U}_{\mathbf{S4}} \end{pmatrix} \begin{pmatrix} \nu_1 \\ \nu_2 \\ \nu_3 \\ \boldsymbol{\nu}_4 \end{pmatrix}$$

- Consider experiments where $\frac{E}{L} \approx \Delta m^2_{41}$ and $\Delta m^2_{41} >> \Delta m^2_{21}, \Delta m^2_{32}$.
- If we are only sensitive to electron and muon flavours in the detector:

$$\mathrm{U}_{e4}, \mathrm{U}_{\mu 4} \text{ and } \Delta \mathrm{m}^2_{41}$$

$$P(\nu_e \to \nu_e) = 1 - 4(1 - |\mathrm{U}_{e4}|^2)|\mathrm{U}_{e4}|^2 \sin^2(1.27 \Delta \mathrm{m}^2_{41} \frac{L}{E}) \quad (\nu_e \text{ disappearance})$$

$$P(\nu_\mu \to \nu_\mu) = 1 - 4(1 - |\mathrm{U}_{\mu 4}|^2)|\mathrm{U}_{\mu 4}|^2 \sin^2(1.27 \Delta \mathrm{m}^2_{41} \frac{L}{E}) \quad (\nu_\mu \text{ disappearance})$$

$$P(\nu_\mu \to \nu_e) = 4|\mathrm{U}_{e4}|^2|\mathrm{U}_{\mu 4}|^2 \sin^2(1.27 \Delta \mathrm{m}^2_{41} \frac{L}{E}) \quad (\nu_e \text{ appearance})$$

Appearance and disappearance signals are related!

Radiochemical Experiments

- The SAGE and GALLEX experiments both observed a deficit of electron neutrinos with radioactive isotope sources.

Reactor Experiments

- 3.5% deficit of electron anti-neutrinos in several reactor experiments.

Accelerator Experiments

- Excess of electron neutrinos and anti-neutrinos in the LSND and MiniBooNE experiments.

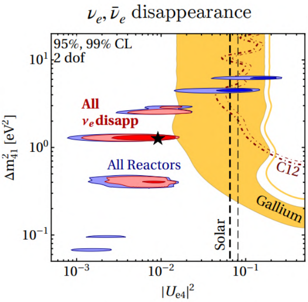

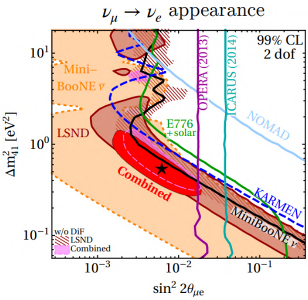

Radiochemical Experiments

- The SAGE and GALLEX experiments both observed a deficit of electron neutrinos with radioactive isotope sources.

Reactor Experiments

- 3.5% deficit of electron anti-neutrinos in several reactor experiments.

Accelerator Experiments

- Excess of electron neutrinos and anti-neutrinos in the LSND and MiniBooNE experiments.

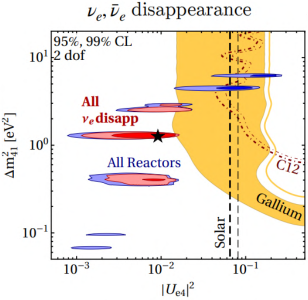

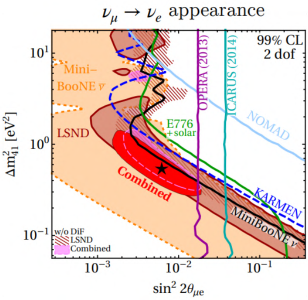

Hints towards sterile neutrino,
but tension in global fits remains.

1. LSND sees $\bar{\nu}_e$ appearance from a well understood $\bar{\nu}_\mu$ neutrino source [14].

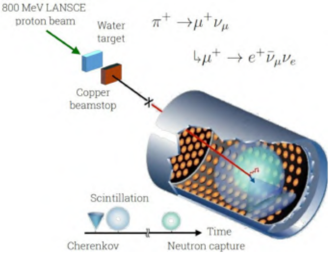

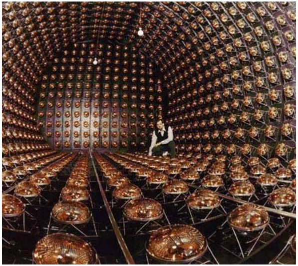

1. **LSND** sees $\bar{\nu}_e$ appearance from a well understood $\bar{\nu}_\mu$ neutrino source [14].

2. **MiniBooNE** has different L, E, but similar $L/E \sim$ LSND $\mathcal{O}(1\,\mathrm{m\,MeV^{-1}})$.

The MiniBooNE Low-Energy Excess [1]

- In Fermilab's Booster Neutrino Beam, since 2002.
- Mineral Oil Cherenkov detector.
- Doubled statistics in 2018.
- Excess of events observed, as in LSND.

MiniBooNE Detector

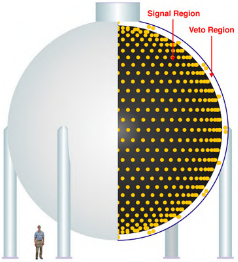

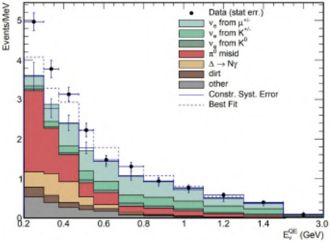

Anomalies in Accelerator Experiments

1. **LSND** sees $\bar{\nu}_e$ appearance from a well understood $\bar{\nu}_\mu$ neutrino source [14].

2. **MiniBooNE** has different L, E, but similar $L/E \sim$ LSND $\mathcal{O}(1\,\mathrm{m\,MeV}^{-1})$.

The MiniBooNE Low-Energy Excess [1]

- In Fermilab's Booster Neutrino Beam, since 2002.
- Mineral Oil Cherenkov detector.
- Doubled statistics in 2018.
- Excess of events observed, as in LSND.

3. **MicroBooNE**: same L, E with different technology.

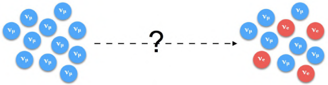

A step back in time: The LSND Exepriment

Liquid Scintillator Neutrino Detector at Los Alamos

- Data-taking 1993-1998.
- $\bar{\nu}_\mu$ from μ^+ Decay at rest.
- 3.8σ excess consistent with ν_e appearance ($\Delta m \approx 1\,\mathrm{eV}^2$).

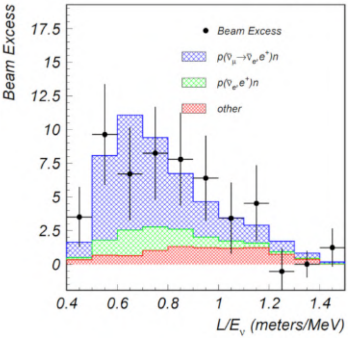

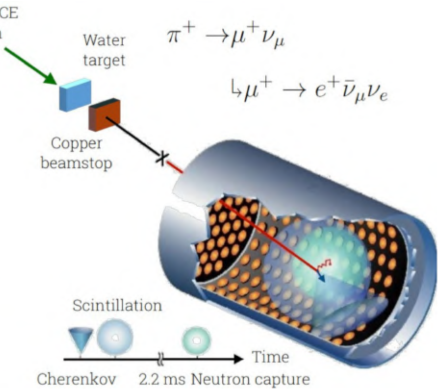

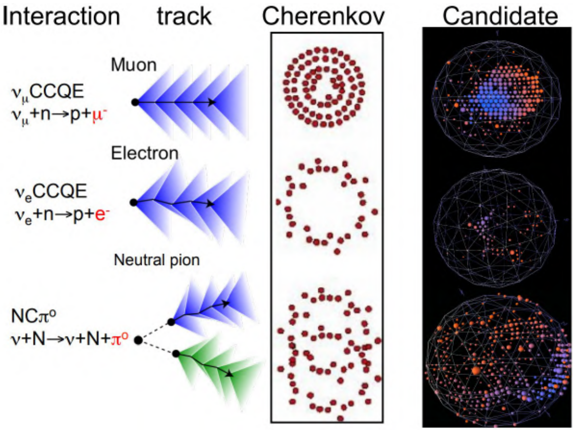
Interaction
track
Cherenkov
Candidate
Muon
ν_μCCQE
ν_μ+n→p+μ^-
Electron
ν_eCCQE
ν_e+n→p+e^-
Neutral pion
NCπ^o
ν+N→ν+N+π^o

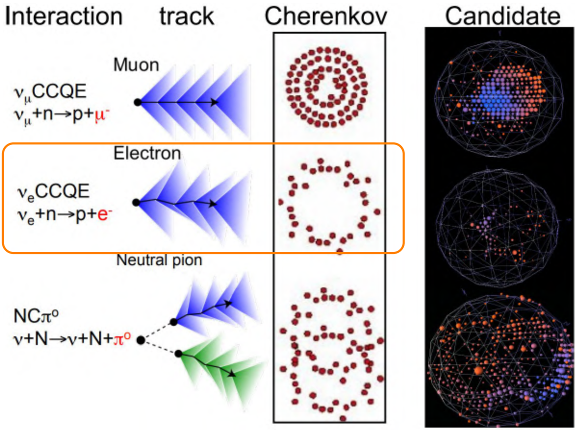

MiniBooNE sees an **excess of low energetic electromagnetic events**.
No discrimination between a single photon and an electron + insensitive to protons.
The **origin of the excess remains unclear**.

Liquid Argon Time Projection Chamber

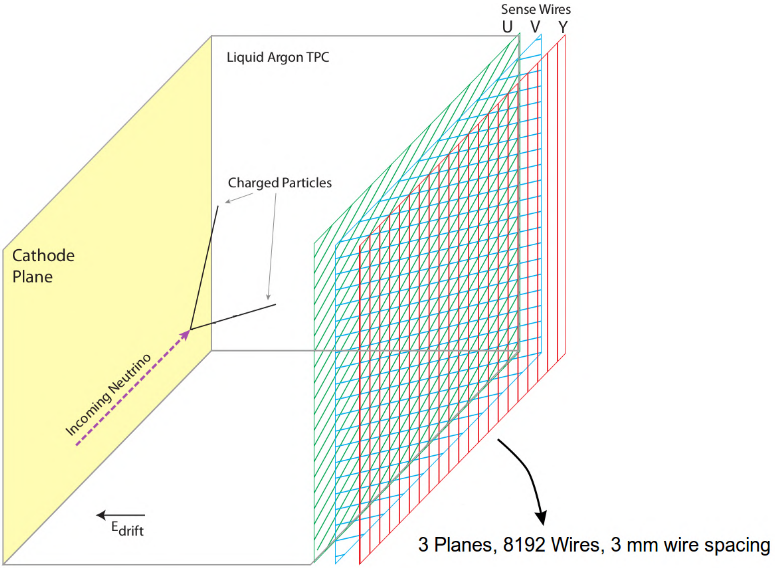

Liquid Argon Time Projection Chamber

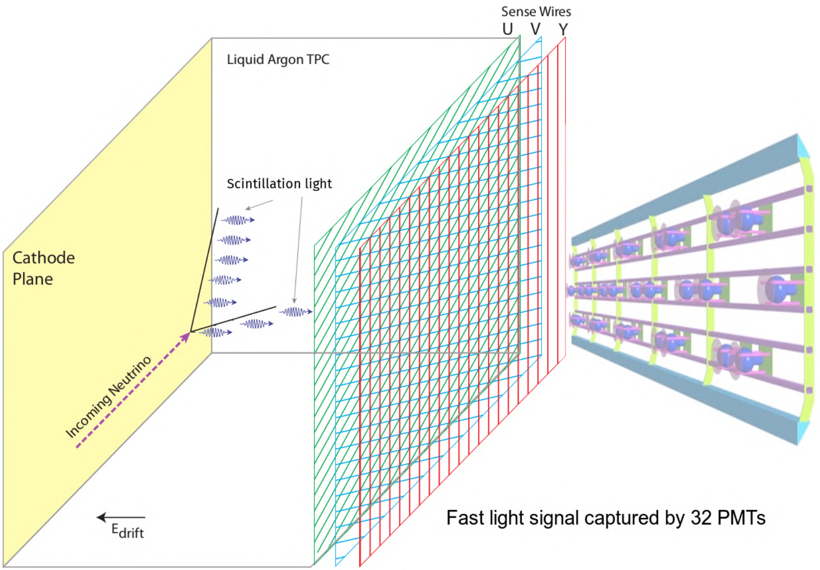

Liquid Argon Time Projection Chamber

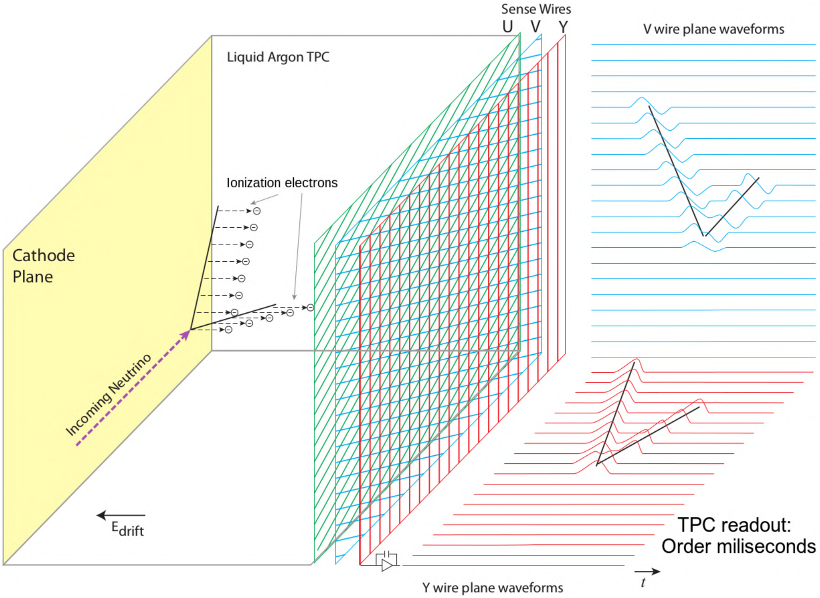

MicroBooNE Data Event

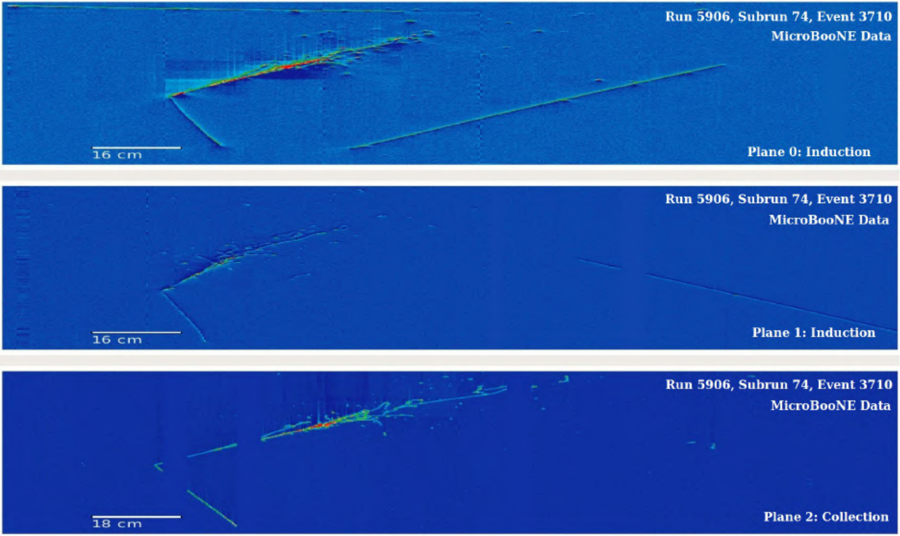

MicroBooNE Data Event

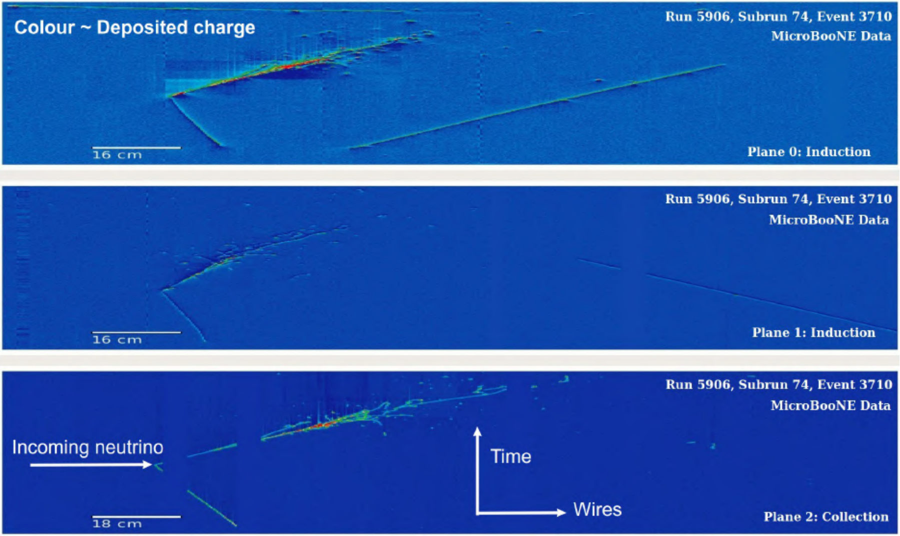

MicroBooNE Data Event

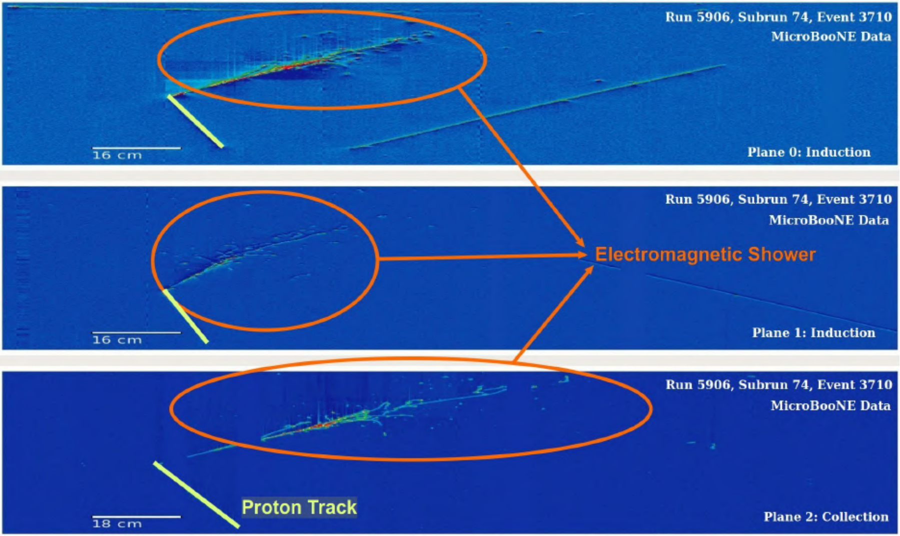

Two possible models to explain the low-energy excess

Electron-like Search

Electron neutrinos from oscillation

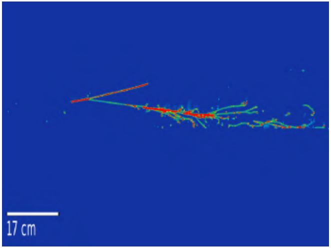

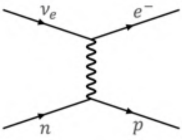

Photon-like Search

Neutral current $\Delta \to N\gamma$

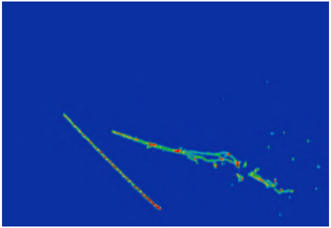

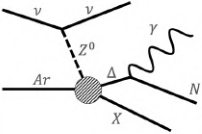

Unfolding the MiniBooNE excess (MICROBOONE-NOTE-1043-PUB)

Electron-like Search

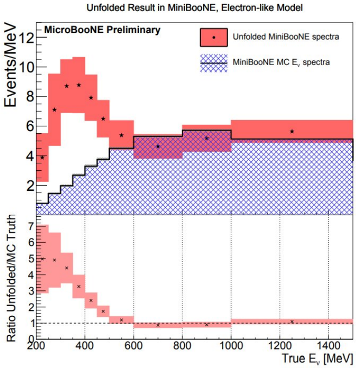

Photon-like Search

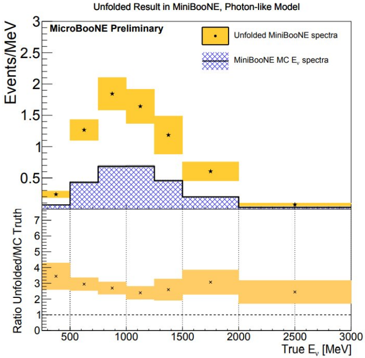

Events contain a lot of cosmic charge deposits

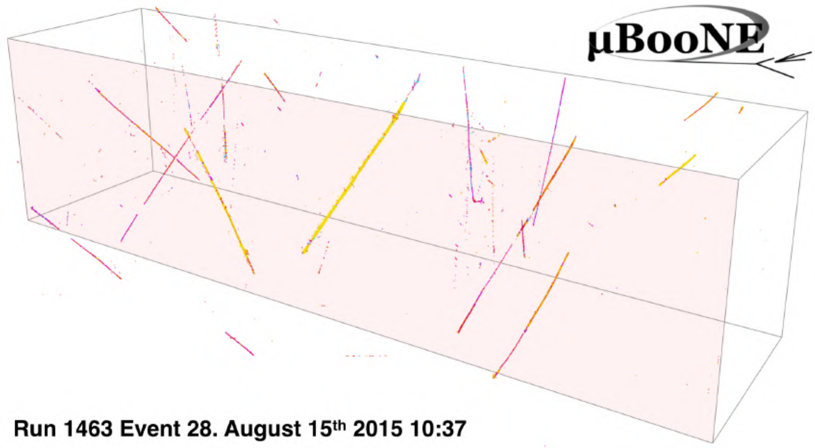

Three different reconstruction approaches in MicroBooNE:

- First time **fully automatic** event reconstruction used in LArTPC.
- Serve to **cross-check** each other in parallel efforts.
- Essential build-up of **expertise for DUNE, SBND and ICARUS**.

WireCell Tomographic Imaging

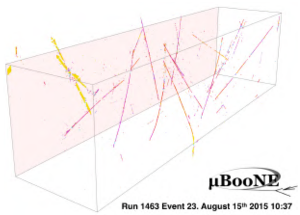

MICROBOONE-NOTE-1040-PUB

Deep-Learning

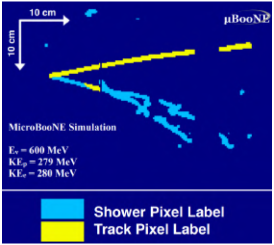

Phys. Rev. D 99, 092001 [15]

Pandora Multi-Algorithm

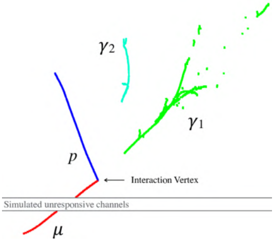

Eur. Phys. J. C. 2019. [8]

ν_μ and ν_e have much in common:

- **Flux**: both species of neutrinos come from the same beam, from decays of the same populations of hadrons.
- **Cross-Section**: both neutrinos interact with argon nuclei.
- **Detector**: systematic detector effects affect different channels in the same way.

Strong **correlation** between the ν_μ and ν_e cross-section **at low energies**.

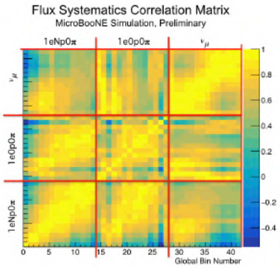

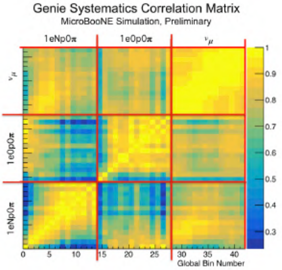

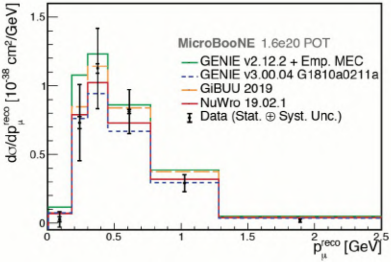

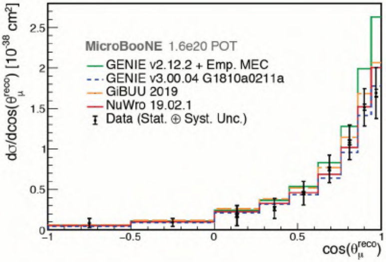

First Cross-section results from MicroBooNE

- Using Run 1 data-set, ≈13 % of total POT collected.
- Measurement of Inclusive Muon Neutrino Charged-Current Differential Cross Sections on Argon [2]
- Measurement of ν_μ Charged-Current π^0 Production on Argon [3]

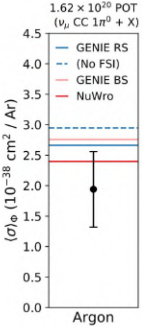

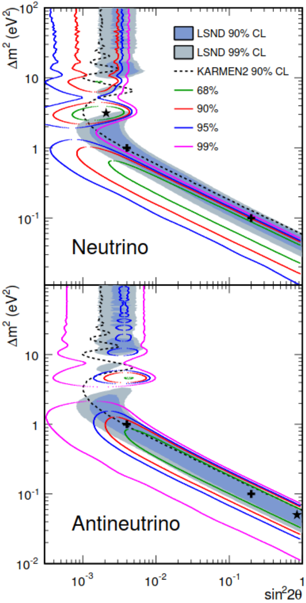
LSND 90% CL
LSND 99% CL
KARMEN2 90% CL
68%
90%
95%
99%
Neutrino
Antineutrino
Δm^2 (eV^2)
10^2
10
1
10^{-1}
10^{-2}
10^{-3}
10^{-2}
10^{-1}
1
$\sin^2 2\theta$

The Short Baseline Programme (SBN) at Fermilab [4]

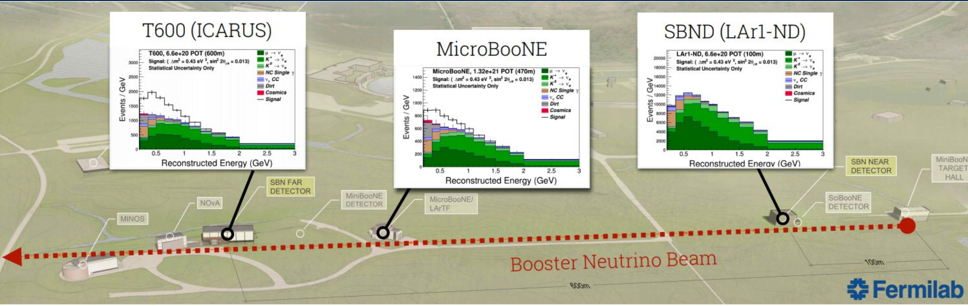

Sensitivity to the short-baseline anomaly

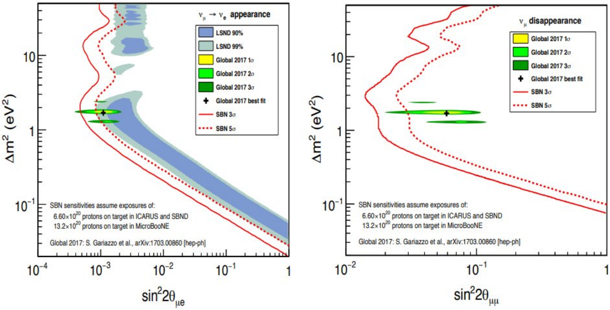

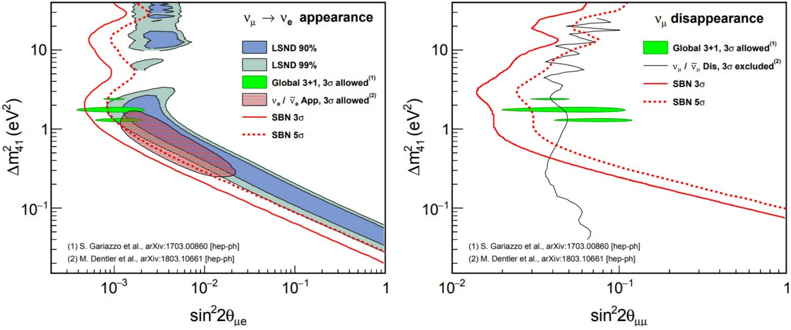

Figure 7

SBN 3σ (solid red line) and 5σ (dotted red line) sensitivities to a light sterile neutrino in the $\nu_\mu \rightarrow \nu_e$ appearance channel *(left)* and $\nu_\mu \rightarrow \nu_\mu$ disappearance channel *(right)*. For comparison, the LSND preferred region at 90% C.L. (shaded blue) and 99% C.L. (shaded gray) is presented (19). Moreover, the global ν_e appearance (shaded red) and global ν_μ disappearance (black line) 3σ regions from Ref. (33) are also included. Finally, the 3σ global best fit regions from Ref. (35) are shown in green. The sensitivities are reproduced from the SBN proposal (15).

ν_μ and ν_e have much in **common**:

- **Flux**: both species of neutrinos come from the same beam, from decays of the same populations of hadrons.

Dominant production modes:

$\nu_\mu : \pi^+ \to \mu^+ \nu_\mu$ 94%

$\nu_e : \mu^+ \to e^+ \nu_e \bar{\nu}_\mu$ 52%

Other sources of systematic uncertainty:

- **Cross-Section**: both neutrinos interact with argon nuclei.
- **Detector**: systematic detector effects affect different channels in the same way.

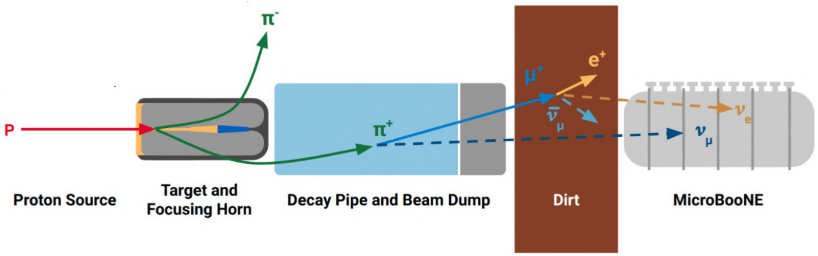

- ν_μ flux peaks at ≈0.8 GeV.
- Small ν_e component: ≈0.57 %.

→ ν_e's from Kaons at lowest energies can be constrained by high energy ν_μ's.